Applied Mathematical Modelling 33 (2009) 4097–4119

Contents lists available at ScienceDirect

Applied Mathematical Modelling

journal homepage: www.elsevier.com/locate/apm

Reduced order fully coupled structural–acoustic analysis via implicit moment matching

R. Srinivasan Puri [a,*], Denise Morrey [a], Andrew J. Bell [a], John F. Durodola [a], Evgenii B. Rudnyi [b], Jan G Korvink [b]

[a] School of Technology, Oxford Brookes University, Wheatley Campus, Wheatley, Oxford OX33 1HX, United Kingdom
[b] IMTEK – Department of Microsystems Engineering, University of Freiburg, Georges-Koehler-Allee 103, D-79110 Freiburg, Germany

ARTICLE INFO

Article history:
Received 23 October 2007
Received in revised form 2 February 2009
Accepted 16 February 2009
Available online 10 April 2009

Keywords:
Fully coupled structural–acoustic analysis
Krylov subspaces
Arnoldi algorithm
Implicit moment matching

ABSTRACT

A reduced order model is developed for low frequency, undamped, fully coupled structural–acoustic analysis of interior cavities backed by flexible structural systems. The reduced order model is obtained by applying a projection of the coupled system matrices, from a higher dimensional to a lower dimensional subspace, whilst preserving essential properties of the coupled system. The basis vectors for projection are computed efficiently using the Arnoldi algorithm, which generates an orthogonal basis for the Krylov Subspace containing moments of the original system. The key idea of constructing a reduced order model via Krylov Subspaces is to remove the uncontrollable, unobservable and weakly controllable, observable parts without affecting the transfer function of the coupled system. Three computational test cases are analyzed, and the computational gains and the accuracy compared with the direct inversion method in ANSYS.

It is shown that the reduced order model decreases the simulation time by at least one order of magnitude, while maintaining the desired accuracy of the state variables under investigation. The method could prove as a valuable tool to analyze complex coupled structural–acoustic systems, and their subsequent optimization or sensitivity analysis, where, in addition to fast analysis, a fine frequency resolution is often required.

1. Introduction

In a modern passenger vehicle or a commercial aircraft the noise, vibration and harshness (NVH) performance is one of the key parameters which the customer uses to assess product quality. In order to gain competitive advantage, manufacturers are continually striving to reduce NVH levels. As a result, design engineers often seek to evaluate the low frequency NVH behavior of automotive/aircraft interiors using coupled finite element-finite element (FE/FE) or finite element-boundary element (FE/BE) discretized models. Due to the coupling between the fluid and structural domains in the coupled displacement/pressure (u/p) FE/FE formulation [1–3], the resulting mass and stiffness matrices are no longer symmetrical. In addition to this, at least 6–8 linear elements per wavelength are required to give reasonable prediction accuracy for structural–acoustic problems [4–7]. This can result in huge model sizes for higher frequency analysis, and hence a significant increase of computational time and expense. Furthermore, this presents as a major problem where optimization is required, especially when there are a large number of design variables to be optimized. Therefore, generation of compact models, for fast coupled structural–acoustic analysis is of great interest to the NVH community.

* Corresponding author.
E-mail address: srinivaspuri@gmail.com (R. Srinivasan Puri).

0307-904X/$ - see front matter © 2009 Published by Elsevier Inc.
doi:10.1016/j.apm.2009.02.016

Alternative FE/FE formulations leading to positive-definite, symmetric matrices do exist, and can be classified by unknown fluid variables taking the form of velocity potential [8,9], a combination of velocity potential and sound pressure level [10], displacements in the fluid [11] and a combination of displacements and pressures [12]. However, these formulations encounter new problems such as spurious rotational modes, increase in dimension of the problem size or involves solving a complex dynamic matrix for an undamped coupled structural–acoustic problem. Such problems with these other formulations have resulted in the *Eulerian* (u/p) formulation [1–3] being adopted as the most appropriate prediction technique [7], and being widely employed in commercially available FE codes such as ANSYS, MSC/Nastran, DSS ABAQUS, LMS SYSNOISE.

The two most popular approaches to reduce the computational time of such coupled problems are mode superposition and the component mode synthesis (CMS) methods. The former method uses the dominant natural frequencies and mode shapes, extracted from a normal modal analysis and the response is assumed to be a linear combination of these modes. However, the standard mode superposition method, suffers from four major drawbacks: (a) The computation of coupled modes using a non-symmetric eigen-solver tends to be computationally very demanding [13]. (b) The second drawback is the treatment of damping. For well damped structures, a spatially distributed damping – often varying with frequency, has to be utilised [14]. (c) If a structural–acoustic optimization problem in a particular frequency band is considered, there exists the problem of only the higher order modes being truncated, leading to unwanted estimation of lower order modes repeatedly [15] and (d) The number of modes required to represent the frequency band under investigation is often an approximate guess of between $1.2\omega_E$ to $2\omega_E$ where ω_E is the upper frequency range [16]. In the modal synthesis or the CMS type approach, the system is divided into different components (structure and fluid), and the uncoupled normal modes from a symmetric eigenvalue problem are calculated. This set can then be treated as vectors for projection in the standard modal superposition model. However, the efficiency of the CMS type formulation for coupled structural–acoustic problems in reducing model size is poor, since a large number of acoustic modes are required to enforce displacement continuity along the fluid–structure interface. This is mainly due to the fact that the modes of the uncoupled acoustic model have a zero normal fluid displacement along the fluid–structure coupling interface. Therefore, for an accurate representation of the near-field effects in the vicinity of the fluid–structure coupling interface a large number of high-order modes in the acoustic modal basis is required, resulting in slow convergence of the coupled problem. This has been numerically demonstrated for a 1D tube example [6]. Further, the effect of the kept (retained) *dry* modes is critical to the convergence in the uncoupled modal basis method, especially for *strongly coupled* problems (e.g. presence of heavy fluid) [17–19].

The restriction of these two methods has left NVH engineers with a very limited number of tools for the numerical analysis of vehicle/aerospace interior noise prediction problems, and hence they are often forced to resort to mixed experimental–numerical approaches [20]. Other approaches to reduce computational time for structural–acoustic problems include the use of symmetrization techniques [21,17,19,22], geometric mesh skinning, the variation to the CMS approach namely the Automated Multi-level Substructuring [23,22], generation of Ritz vectors [21], use of acoustic influence co-efficients from BE models [24], truncated FE/FE analysis [15], the patented Acoustic Transfer Vector (ATV) method [25] and the use of *look-ahead* Lanczos process for symmetric matrices [26,27], to name a few. The reader is referred to the reviews by [4,17,14,28–31] for a description of some of the above mentioned approaches.

More recently, model order reduction (MOR), via implicit moment matching, has received considerable attention among mathematicians and the circuit simulation community [32,33]. It has been shown in various engineering applications [34–38], that the time required to solve reduced order models via implicit moment matching is significantly reduced when compared to solving the original higher dimensional problem and whilst maintaining the desired accuracy of the solution. The aim of MOR is to construct a reduced order model, from the original higher dimensional problem, which gives a faithful representation of the system input/output behavior (i.e. the transfer function) at particular points in the frequency domain. The reduction is achieved by applying a projection from a higher order to a lower order space using a set of Krylov Subspaces, generated by the Arnoldi algorithm. Additionally, the reduced model preserves certain essential properties such as maintaining the second order form and stability. Therefore, it would be possible to carry out investigations on the original system by replacing it with a reduced order model and undertake design modifications for a much smaller computational cost and time.

The paper focuses on the application of such Krylov-based MOR techniques to undamped, fully coupled structural–acoustic problems. The remainder of the paper is laid out as follows: In Section 2 the general framework for model order reduction for second order systems and its application to the coupled structural–acoustic problem is described. The Arnoldi algorithm adapted for model order reduction for the fully coupled structural–acoustic problem is presented. In Section 3 three numerical examples are solved by the direct approach using ANSYS finite element (FE) code [39], and by MOR via the moment matching Arnoldi approach. Simple models for error estimates and thus the convergence properties of MOR via the Arnoldi process are discussed. Further, the accuracy and computational times from the numerical test cases considered in this paper are discussed. Finally, Section 4 concludes the paper with a short discussion of the potential applications of MOR in structural acoustics, and future recommendations.

2. Model order reduction for second order systems

After discretization in space of a general mechanical system model, one obtains a system of ordinary differential equations of second order in matrix form as follows [40]:

$$\begin{aligned}&[\mathbf{M}]\ddot{x}(t) + [\mathbf{C}]\dot{x}(t) + [\mathbf{K}]x(t) = Fu(t),\\ &y(t) = L^T x(t),\end{aligned} \tag{1}$$

where t is the time variable, $x(t)$ is a vector of state variables, $u(t)$ is the input force vector, and $y(t)$ the output measurement vector which is used to extract the desired state variable(s) $x(t)$. The matrices $\mathbf{M}$, $\mathbf{C}$ and $\mathbf{K} \in \Re^{N\times N}$ are the mass, damping and stiffness matrices, respectively. N is the state-space dimension. $F \in \Re^{N\times p}$ and $L \in \Re^{N\times m}$ are the input distribution and output scattering matrix. The matrix $L^T \in \Re^{N\times N}$ is a square identity matrix in the case of a complete output of states $x(t)$ being required. Assuming harmonic excitation of the form $Fu(t) = Fe^{j\omega t} = \{F\}$, a response of $\{x\} = \{x_{max}e^{j\phi}\}e^{j\omega t}$, where ϕ is the phase shift and removing the time dependency term $e^{j\omega t}$ on both sides of Eq. (1) yields:

$$\begin{aligned}&[-\omega^2[\mathbf{M}] + j\omega[\mathbf{C}] + [\mathbf{K}]]\{x\} = \{F\},\\ &y(\omega) = L^T x(\omega),\end{aligned} \tag{2}$$

where ω denotes the circular frequency, and $\{x\}$ and $\{F\}$ denote complex vectors of state variables and inputs to the system, respectively.

Ignoring damping, Eq. (2) becomes:

$$\begin{aligned}&[-\omega^2[\mathbf{M}] + [\mathbf{K}]]\{x\} = \{F\},\\ &y(\omega) = L^T x(\omega).\end{aligned} \tag{3}$$

The principle of model order reduction is to find a lower dimensional subspace $[V] \in \Re^{N\times q}$, such that:

$$x \approx [V]z + \varepsilon, \tag{4}$$

where $z \in \Re^q$ and $q \ll N$, such that the steady state or time-dependent behavior of the original higher dimensional state vector can be well approximated by the projection matrix $[V]$ in relation to a considerably reduced vector of order q, with the exception of a small error, ε. Once the projection matrix V is found, the original equation (2) is projected onto it. The projection produces a reduced set of system equations, in second order form, as follows:

$$\begin{aligned}&[-\omega^2[\mathbf{M}_r] + [\mathbf{K}_r]]\{z\} = \{F_r\},\\ &y_r(\omega) = L_r^T z(\omega),\end{aligned} \tag{5}$$

where the subscript r denotes the reduced matrix and:

$$[\mathbf{M}_r] = [V^T][\mathbf{M}][V]; \quad [\mathbf{K}_r] = [V^T][\mathbf{K}][V]; \quad \{F_r\} = V^T\{F\}; \quad L_r^T = L^T V. \tag{6}$$

It is worth noting that $y_r(\omega) \approx y(\omega)$, with the exception of the small error ϵ.

Due to its low dimensionality, the solution to equation (5) is much faster than the original higher dimensional model.

There exist several methods to choose $[V]$. In this work, we choose the projection matrix $[V]$ to be a Krylov Subspace in order to provide the moment matching property [41]. Given a matrix $[A]$ and a vector g, a Krylov Subspace of order q is defined by:

$$\mathscr{K}_q(A, g) = span(g, Ag, \ldots, A^{q-1}g), \tag{7}$$

where g is called the starting vector and $Ag, \ldots, A^{q-1}g$ are called basis vectors. A straightforward application of the Krylov Subspace methods for second order system produces a reduced order system which is of first order or the so-called *state space* model. This is not so desirable because the properties of the matrices and the physical significance of the original system could be destroyed. In order to avoid this problem, a modified version of the Arnoldi algorithm has been proposed [41].

2.1. Model order reduction for coupled structural–acoustic systems

For an interior, fully coupled structural–acoustic case and considering the enclosed acoustic fluid domain, D, the boundary surface $D_a (D_a = D_s \cup D_v \cup D_p \cup D_z)$ contains an elastic surface D_s as shown in Fig. 1. Considering the boundary surface, four different types of boundary conditions can be applied on D_a of the bounded fluid domain D:

(a) Applied normal velocity on $D_v : v_n = (j/\rho_0\omega) \cdot (\partial p/\partial n)$.
(b) Normal velocity continuity on $D_s : v_n = (j/\rho_0\omega) \cdot (\partial p/\partial n) = j\omega u_n = \bar{v}_n$.
(c) Applied pressure on $D_p : p = \bar{p}$.
(d) Applied normal impedence on $D_z = \overline{Z} \cdot v_n$,where $\bar{p}$ is a prescribed pressure function, $\bar{v}$ is the prescribed normal velocity function, $\overline{Z}$ is the prescribed normal impedence function, u_n is the normal structural displacement and n denotes the normal to the boundary surface of D. The normal velocity continuity condition enforces the *two-way* fluid–structure coupling such that the normal fluid velocity equals the normal structural velocity at the coupling interface, often referred to as the *wetted surface*.

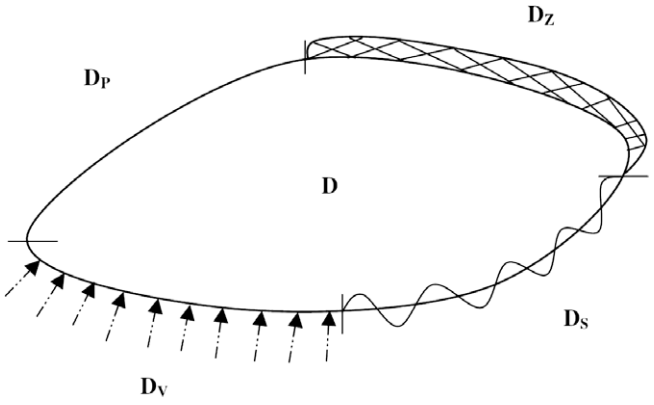

Fig. 1. Interior coupled structural–acoustic system.

For simple harmonic motion, the governing equation for sound pressure p inside the fluid domain for the uncoupled acoustic case is the reduced Helmholtz equation [42]:

$$\nabla^2 p + k^2 p = 0, \tag{8}$$

where ∇^2 is the Laplacian operator, p is the acoustic pressure, and k is the wave number ($k = \omega/c$), ω is the circular frequency, and c is the speed of sound in the acoustic medium. A finite element discretization of Eq. (8), taking into account the acoustic source excitation (volume velocity/acceleration), for the acoustic discretization, in terms of global shape functions for the nodal pressure p, results in [7]:

$$[-\omega^2[\mathbf{M}_a] + j\omega[\mathbf{C}_a] + [\mathbf{K}_a]]\{p\} = \{F_a\}, \tag{9}$$

where the subscript a denotes the matrix terms belonging to the acoustic domain.

Turning then to the enclosing structure, a forced response analysis of the uncoupled structure in the frequency domain is quite straightforward [40] and then accounting for the force loading of the fluid pressure on the structure and enforcing the normal structural, fluid velocity continuity condition on Eq. (9), along the fluid–structure interface or the so-called *wetted surface* leads to the well known combined *Eulerian* displacement–pressure (u/p) formulation for the structural–acoustic model as a whole [1–3]:

$$\begin{bmatrix} M_s & 0 \\ M_{fs} & M_a \end{bmatrix} \begin{Bmatrix} \ddot{u} \\ \ddot{p} \end{Bmatrix} + \begin{bmatrix} C_s & 0 \\ 0 & C_a \end{bmatrix} \begin{Bmatrix} \dot{u} \\ \dot{p} \end{Bmatrix} + \begin{bmatrix} K_s & K_{fs} \\ 0 & K_a \end{bmatrix} \begin{Bmatrix} u \\ p \end{Bmatrix} = \begin{Bmatrix} F_s \\ F_a \end{Bmatrix} \tag{10}$$

and,

$$y(t) = L^T \begin{Bmatrix} u \\ p \end{Bmatrix},$$

where M_s is the structural mass matrix, M_a is the acoustic mass matrix; K_s is the structural stiffness matrix, K_a is the acoustic stiffness matrix; M_{fs} is the coupling mass matrix, and K_{fs} is the coupling stiffness matrix; u denotes the structural displacements, p denotes the nodal pressures in the fluid domain, and F_s and F_a denote the force(s) on the structural domain and constrained acoustic pressure degrees of freedom (DOF's) or purely acoustic excitation, in the form of volume acceleration belonging to the fluid domain respectively. As mentioned earlier, the matrix L^T is the output scattering matrix, of dimension $N \times N$, which is a square identity matrix to restore a complete output of states, which in this case the displacements and pressures corresponding to the structural and fluid domain, respectively. It is worth noting that, in the case where fewer outputs are required, the matrix L^T is permuted to form $1's$ only at required output DOF's. Thus, if an average value of the desired states are sought, the diagonal entries of the square matrix L^T would be $1/N$, where, N is the dimension of the original higher dimensional model. In this paper, it is assumed that the matrices are real. Constructing reduced order models via Krylov Subspaces, for fully coupled models with different forms of damping within the framework of model order reduction via implicit moment matching will be shortly discussed in Section 4.

Comparing Eq. (10) to a one-way coupled analysis, the coupled formulation results in unsymmetric stiffness and mass matrices given by the terms K_{fs} and M_{fs} respectively. It is worth mentioning that Eq. (10) is unsymmetric due to the fact that the force loading of the fluid on the structure is proportional to the pressure, given by the term K_{fs} in the stiffness matrix, and the force loading of the structure on the fluid is proportional to acceleration, given by the term M_{fs} in the mass matrix [6,7].

Ignoring damping for the structure and fluid, the coupled equations become:

$$\begin{aligned} &\left(\begin{bmatrix} K_s & K_{fs} \\ 0 & K_a \end{bmatrix} - \omega^2 \begin{bmatrix} M_s & 0 \\ M_{fs} & M_a \end{bmatrix} \right) \cdot \begin{Bmatrix} u \\ p \end{Bmatrix} = \begin{Bmatrix} F_s \\ F_a \end{Bmatrix} \\ &y(\omega) = L^T \begin{Bmatrix} u \\ p \end{Bmatrix} \end{aligned} \tag{11}$$

It can be seen that Eq. (11) is similar to Eq. (2) except that there is explicitly more than one output in the case of (11). These are displacements of the structure and pressure levels at nodes inside the fluid. From a MOR point of view, this is not of any concern, since the projection matrix $[V]$ is related to the generalized co-ordinates, and is not directly related to nodal degrees of freedom. In this case, the approximation becomes:

$$\begin{Bmatrix} u \\ p \end{Bmatrix} = \{x\} \approx Vz + \varepsilon. \tag{12}$$

This form is often denoted as the *change of state co-ordinates*.

Ignoring damping and rewriting Eq. (10) using Laplace transforms, in terms of the input $U(s)$ and the output $Y(s)$ which are related by the *transfer function* $H(s) = [Y(s)/U(s)]$, gives:

$$H(s) = L^T(s^2 M_{sa} + K_{sa})^{-1} F_{sa}, \tag{13}$$

where $(s^2 M_{sa} + K_{sa})$ is called the *characteristic polynomial matrix* and the matrices:

$$K_{sa} = \begin{bmatrix} K_s & K_{fs} \\ 0 & K_a \end{bmatrix}, \quad M_{sa} = \begin{bmatrix} M_s & 0 \\ M_{fs} & M_a \end{bmatrix}, \quad \text{and} \quad F_{sa} = \begin{Bmatrix} F_s \\ F_a \end{Bmatrix}.$$

Expanding Eq. (13) using the Taylor series about $s = 0$ results in:

$$H(s) = L^T(s^2 K_{sa}^{-1} M_{sa} + I)^{-1} K_{sa}^{-1} F_{sa}, \tag{14}$$

$$H(s) = \sum_{i=0}^{\infty} (-1)^i L^T (K_{sa}^{-1} M_{sa})^i K_{sa}^{-1} F_{sa} s^{2i}, \tag{15}$$

$$H(s) = \sum_{i=0}^{\infty} m_i s^{2i}, \tag{16}$$

where $m_i = (-1)^i L^T (K_{sa}^{-1} M_{sa})^i K_{sa}^{-1} F_{sa}$ are called the moments of $H(s)$.

The transfer function described in Eq. (13), can be represented as a rational function:

$$H(s) = \frac{N(s)}{D(s)}, \tag{17}$$

where the numerator and denominator, given by $N(s)$ and $D(s)$, are both polynomials in s. A qth order Padé approximation of the transfer function, can be defined as:

$$H_q(s) = \frac{b_{q-1} s^{q-1} + \cdots + b_1 s + b_0}{a_q s^q + a_{q-1} s^{q-1} + \cdots + a_1 s + 1}. \tag{18}$$

Now, the $2q$ co-efficients in (18), namely the co-efficients of $N(s)$ and $D(s)$ can be selected to match the $2q$ terms of the Taylor series expansion of the transfer function in (16), denoted by:

$$H(s) = \sum_{i=0}^{\infty} m_i s^{2i}. \tag{19}$$

By matching some of these moments about $s = 0$, the reduced order model can be constructed, as it directly relates the input to the output of the system. One approach to construct the qth order Padé approximation, is to explicitly compute the moments m_i, using:

$$m_i = (-1)^i L^T (K_{sa}^{-1} M_{sa})^i K_{sa}^{-1} F_{sa} \tag{20}$$

and then generate the co-efficients of the polynomials in Eq. (18). However, computing Padé approximants using explicit moment computations, is done using the Asymptotic Waveform Evaluation (AWE), and suffers from fundamental numerical limitations and is numerically unstable [43,44]. Each run of AWE generates only a small number of accurate poles and zeros. The main reason for the instability in AWE, is the formulation of explicit computation of moments given in Eq. (20).

By setting $[A] = K_{sa}^{-1} M_{sa}$ and $g = K_{sa}^{-1} F_{sa}$, the computation of moments can be achieved by generating two sets of vectors [45]:

$$g, Ag, (A)^2 g, \ldots, (A)^{q-1} g \tag{21}$$

and,

$$L, (A)^T L, ((A)^T)^2 L, \ldots, ((A)^T)^{q-1} L \tag{22}$$

and computing the inner products to form the moments of the transfer function:

$$m_{2i} = ((A^T)^i L)^T \cdot (A^i g), \quad m_{2i+1} = ((A^T)^i L)^T \cdot (A^{i+1} g). \tag{23}$$

The main problem in this method is that the vectors described by Eqs. (21) and (22) quickly converge to the right and left eigenvector corresponding to the dominant eigenvalue of A, and so contain only part of the spectrum of A, which is often not sufficient to approximate the original transfer function.

It can be also be seen however, that the vectors spanning the space in Eqs. (21) and (22) are none other than the qth right and left Krylov Subspaces given by:

$$\mathscr{K}_q^r(A,g) = span(g, Ag, \ldots, A^{q-1}g) \tag{24}$$

which is called the qth right Krylov Subspace induced by A and g, and,

$$\mathscr{K}_q^l(A^T,L) = span(L, A^TL, \ldots, (A^T)^{q-1}L) \tag{25}$$

which is called the qth left Krylov Subspace induced by A and L. The inner products of these two expressions lead to the same moments of the transfer function as given in Eq. (23). However, the vectors belonging to the Krylov Subspace quickly become linearly dependent and there is a rapid accumulation of rounding errors, and hence these are not suitable in general as basis vectors. Instead, a more suitable and stable set of basis vectors can be constructed using vectors v and w, given by:

$$v_1, v_2, v_3, \ldots, v_q \quad \text{and} \quad w_1, w_2, w_3, \ldots, w_q, \tag{26}$$

where v and w are column vectors stored in matrices $[V]$ and $[W]$, such that:

$$\mathscr{K}_q^r(A,g) = span(v_1, v_2, v_3, \ldots, v_q) \tag{27}$$

and,

$$\mathscr{K}_q^l(A^T,L) = span(w_1, w_2, w_3, \ldots, w_q). \tag{28}$$

Now, the direct computation of moments via (21) and (22) can be avoided, and the so-called *modified moments* can be computed as [45]:

$$w_i^T v_i \quad \text{and} \quad w_i^T A v_i, \quad i = 1, 2, \ldots, q. \tag{29}$$

It is worth mentioning that, the *modified moments* contain the same information as the moments in (23), and infact for each $i = 1, 2, \ldots, 2q-1$, the ith moment can be expressed as a suitable linear combination of Eq. (29). In short, if the projection matrix $[V]$ is chosen from a Krylov Subspace of dimension q,

$$\mathscr{K}_q(A,g) = span(g, Ag, \ldots, A^{q-1}g), \tag{30}$$

$$\mathscr{K}_q(K^{-1}M, K^{-1}F) = span(K^{-1}F, K^{-1}MK^{-1}F, \ldots, K^{-1}M^{q-1}K^{-1}F) \tag{31}$$

then, the reduced order model matches $(q+1)$ moments of the higher dimensional model [41]. Loosely speaking, if the qth vector spanning the Krylov sequence is present in matrix V , we match the qth moment of the system. The block vectors $K^{-1}F$ and $K^{-1}M$ can be interpreted as the static deflection due to the force distribution F, and the static deflection produced by the inertia forces associated with the deflection $K^{-1}F$, respectively.

The two main approaches to generate vectors belonging to the Krylov Subspace are the Lanczos and the Arnoldi process. Mathematically speaking, both Lanczos and AWE are equivalent, but their performance vastly differ when implemented on a computer. The classical Lanczos process generates two sets of basis vectors which span the right and left Krylov Subspaces defined in Eqs. (27) and (28) and are bi-orthogonal to match $2q$ moments of the system matrices. However, the Lanczos process terminates prematurely due to $w_i^T v_i \approx 0$. To remedy this problem, a *look-ahead* Lanczos algorithm is proposed [46]. Another major disadvantage of the Lanczos process is that, although the original higher dimensional model is stable and passive, there is no guarantee that the reduced order model generated by projecting the two sets of bi-orthogonal vectors on the original system would generate a stable and passive reduced order model. i.e the stability and passivity of the higher dimensional model is not preserved. A partial Padé via Lanczos has been introduced to counter this problem [47]. Additionally, to match more than one specific output state, a block version of the Lanczos process is required. For this very reason, in this paper, we consider the use of the Arnoldi process to generate vectors containing the *low frequency moments* of the coupled system matrices.

2.2. The Arnoldi algorithm

The two key properties essential for generating vectors belonging to the Krylov Subspace implies [34]:

(a) The low frequency moments of the coupled system are matched without explicit computation of moments.
(b) The procedure is implemented iteratively.

This ensures numerical stability while building up the Krylov Subspace, and that an orthogonal basis is constructed for the given subspace $\mathscr{K}_q(A,g)$. This is done using the Arnoldi algorithm. Given a Krylov Subspace , the Arnoldi algorithm finds a set of vectors with norm one, that are orthogonal to each other, given by:

$$V^T V = I, \tag{32}$$

where the columns of $[V]$ are the basis for the given Krylov sequence and $I \in \Re^{qxq}$ is the identity matrix . Additionally,

$$V^T A V = H_q, \tag{33}$$

where $[H_q]$ is a block upper Hessenberg matrix, and is an orthogonal projection of $[A]$ onto the Krylov Subspace defined in Eq. (24). Fig. 2 gives the simplified single input, single output (SISO) version of implemented Arnoldi algorithm. In comparison with the Lanczos process, it can be observed that the Arnoldi process produces only one sequence of vectors, which span the right Krylov Subspace in Eq. (24), and are orthonormal, as given by:

$$v_i^T v_j = \left\{ \begin{array}{ll} 1 & \text{if } i = j \\ 0 & \text{if } i \neq j \end{array} \right\} \tag{34}$$

for all $1 \leqslant i$ and $j \leqslant q$.

For the fully coupled structural–acoustic formulation described in this work, we now have the following definitions:

$$A = K_{sa}^{-1} M_{sa}, \quad g = K_{sa}^{-1} F_{sa}, \tag{35}$$

$$V^T K_{sa}^{-1} M_{sa} V = H_q \quad \text{and} \quad V^T V = I, \tag{36}$$

$$Colspan(V) = \mathcal{K}_q(K_{sa}^{-1} M_{sa}, K_{sa}^{-1} F_{sa}). \tag{37}$$

The initial dimension of q is chosen such that the input–output behaviour of the coupled system is well represented. This is discussed in some detail in Section 3.2. The discussion of the block version of the algorithm, which is used to generate the Arnoldi vectors for a coupled structural–acoustic system with multiple inputs and multiple outputs (MIMO) is quite involved, and the reader is referred to [33] for a detailed discussion. In short, the block version of the Arnoldi algorithm generates orthogonal vectors belonging to the Krylov Subspace:

Input: System Matrices K_{sa},M_{sa},F_{sa},L^T and q (Number of vectors)

and expansion point s, in this case $s = (\omega_e + \omega_b)/2$

Output: q Arnoldi vectors belonging to the Krylov Subspace

0. Set $v_1^* = g$

1. $^*for\ i = 1 \rightarrow q\ \ ^*do$:

1.1 Deflation Check: $h_{i,i-1} = \|v_i\|$

1.2 Normalization: $v_i = v_i^*/h_{i,i-1}$

1.3 Generation of next vector: $v_{i+1}^* = A v_i$

1.4 Orthogonalization with old vectors $^*for\ j = 1 \rightarrow i\ \ ^*do$:

1.4.1 $h_{j,i} = v_j^T v_{i+1}^*$

1.4.2 $v_{i+1}^* = v_{i+1}^* - h_{j,i} v_j$

2. Discard resulting H_q and project M_{sa},K_{sa},F_{sa},L^T onto V to obtain

reduced system matrices $[M_{rsa}]$,$[K_{rsa}]$,$\{F_{rsa}\}$,L_{rsa}^T

Fig. 2. Complete set-up for SISO/SICO Arnoldi process [32,33].

$$\mathscr{K}_q(A_1, g_1, g_2) = span(g_1, g_2, A_1 g_1, A_1 g_2, \ldots, A^{q-1} g_1, A^{q-1} g_2). \tag{38}$$

Returning to the SISO version of the algorithm as given in Fig. 2, it can be seen that in each step, one vector orthogonal to all previously generated vectors is constructed and normalized. The process is numerically very similar to the modified Gram–Schmidt orthogonalization with the following properties [34,48]:

$$AV_q = V_q H_q + R_q \tag{39}$$

and,

$$A^i g = \|g\| V_q H_q^i e_1 \quad \text{for } i = 0, 1, \ldots, q-1, \tag{40}$$

where R_q is called the residue, and is given by:

$$R_q = h_{q+1,q} v_{q+1} e_q^T, \tag{41}$$

where $h_{q+1,q}$ are the co-efficients of the upper Hessenberg matrix generated at each iteration of the Arnoldi process and e_1 and e_q are the first and the qth standard unit vectors in $\Re^N$. The moments can now be computed as [45,33]:

$$m_i = L^T A^i g = L^T \left(K_{sa}^{-1} M_{sa}\right)^i \left(K_{sa}^{-1} F_{sa}\right). \tag{42}$$

Substituting Eq. (40) in Eq. (42), we have:

$$m_i = L^T A^i g = L^T \|g\| V_q H_q^i e_1 = L^T V_q H_q^i \|g\| e_1, \tag{43}$$

where

$$L^T V_q = L_{rsa}^T, \quad H_q^i = A_{rsa}^i \quad \text{and} \quad \|g\| e_1 = g_{rsa}, \tag{44}$$

where the subscript *rsa* denotes the reduced structural–acoustic matrix. In this case, since only q moments are matched, the approximation is said to be a Padé-type approximant. In some sense, the Arnoldi process trades some optimality to match only q moments of the coupled system matrices, but in turn generates a guaranteed stable and passive reduced order model. i.e. the stability and passivity of the original coupled higher dimensional model is preserved. Once the projection matrix $[V]$ is found, $[H_q]$ is discarded and a Galerkin projection $\prod = VV^T$ on Eq. (11) generates a densely populated reduced order model in second order form, given by:

$$[-\omega^2 [M_{rsa}] + [K_{rsa}]]\{z\} = \{F_{rsa}\}, \tag{45a}$$

$$y_{rsa}(\omega) = L_{rsa}^T z(\omega), \tag{45b}$$

where

$$[M_{rsa}] = V^T M_{sa} V; \quad [K_{rsa}] = V^T K_{sa} V; \quad \{F_{rsa}\} = V^T \{F_{sa}\}; \quad L_{rsa}^T = L^T V. \tag{46}$$

Now, we can also define a reduced order transfer function:

$$H_{rsa}(s) = L_{rsa}^T (s^2 M_{rsa} + K_{rsa})^{-1} F_{rsa} \tag{47}$$

and their associated moments, given by:

$$m_i^{rsa} = (-1)^i L_{rsa}^T A_{rsa}^i g_{rsa}, \tag{48}$$

where m_i^{rsa} are the moments of the reduced order model, and the space spanned by vectors $A_{rsa}^i g_{rsa}$ are the Krylov Subspace vectors. It is worth mentioning that, due to the iterative property of the algorithm, it is also possible to generate a reduced order model of lower dimension than initially specified, by just discarding columns in matrix $[V]$ and subsequently the rows and columns of the reduced matrices. This property is later used to determine the number of vectors needed to accurately represent the system.

From the Arnoldi process shown in Fig. 2, it can be seen that the coupled system matrices $K_{sa}^{-1} M_{sa}$, $K_{sa}^{-1} F_{sa}$ are very important. One of the main aims of performing model order reduction via implicit moment matching is to increase computational efficiency, whilst matching the input to output behavior for the coupled system. However, explicit computation of K_{sa}^{-1} and then using it in the Arnoldi process would lead to a loss of computational efficiency. The remedy to this problem, is to compute the LU factorization of K_{sa} once, and use this in every step of the iteration, thereby solving only triangular linear equations in each iteration of the Arnoldi process.

More precisely speaking, for $s = 0$:

$$K_{sa} = LU \tag{49}$$

and then, for each iteration of the Arnoldi process, which are given by:

$$g_1 = K_{sa}^{-1} F_{sa} \quad \text{and} \quad g_{i+1} = A g_i = K_{sa}^{-1} M_{sa} g_i \tag{50}$$

a back substitution is performed for solving equation (50) by using the following three steps:

(a) First, M_{sa} is multiplied by g_i to give $a = M_{sa}g_i$.
(b) The linear equation $Lb = a$ is forward solved. This is fast, since L is lower triangular. This means $b = L^{-1}a$.
(c) The linear equations $Uc = b$ is forward solved. This is fast, since U is upper triangular. Therefore, $c = L^{-1}U^{-1}M_{sa}g_i = g_{i+1}$, which is the product that is required.

For an expansion point $s \neq 0$, an inverse of $K_{sa} - s^2M_{sa}$ is sought, and therefore, an LU factorization of $K_{sa} - s^2M_{sa}$ is computed and using the LU factors in the above steps (a) to (c), this leads to triangular linear equations being solved at each iteration of the Arnoldi process.

3. Numerical validation

In order to evaluate the accuracy and the computational gains achievable via reduced order modeling, three different test cases were chosen. The first test case was an undamped simply supported aluminium plate backed by a rigid walled cubic cavity. The model is excited in at an off-center node location, and the pressure response computed. In the second test case, undamped frame-panel structure which was used to test new modeling techniques is used for the analysis. The model is excited using a constant unit force across the frequency band of 0–300 Hz and the pressure responses were computed at nodes of interest in the fluid domain. The third test case is a water filled rectangular cavity [18] excited by a unit structural point force across a frequency range of 0–600 Hz. In this test case, both physical vibro-acoustic quantities of interest, namely structural displacement and fluid pressure are specified as outputs.

3.1. Aims and methodology for numerical validation

To evaluate the numerical accuracy and computational gains achieved by employing reduced order models based on moment-matching via the Arnoldi process, the errors of the fluid and structural output quantities and the computational times required to solve the higher dimensional ANSYS model via direct inversion and the reduced order model are compared. In addition to the local error for considered states, two convergence models are used to compute the minimum number of vectors required for convergence. In the first convergence model, a straightforward *true error* and between two models is computed as:

$$\vartheta_{rsa}(s) = \frac{\|H(s) - H_{rsa}(s)\|}{\|H(s)\|}, \tag{51}$$

where $H(s)$ corresponds to the original transfer function, given by, $H(s) = L^T(s^2M_{sa} + K_{sa})^{-1}F_{sa}$ where, the definitions of M_{sa}, K_{sa} and F_{sa} remain the same as in Eq. (13) and $H_{rsa}(s)$ is the reduced order transfer function. Further, a *relative error* between two successive reduced order models q and $q+1$ can be defined as:

$$\hat{\vartheta}_{rsa}(s) = \frac{\|H_{rsa}(s) - H_{rsa+1}(s)\|}{\|H_{rsa}(s)\|} \tag{52}$$

For the reduced order model, the computational time is a combination of three steps: (a) running a Stationary solution and extracting coupled system matrices in ANSYS and *mor4fem* [49]; (b) Generation of Arnoldi vectors and projection to second order form in Mathematica and (c) solution of the reduced order model using the direct LU method. All computations described in this paper were carried out using a Pentium 3 GHz, Windows XP, 2 GB RAM machine.[1]

3.1.1. Test Case No. 1: 3D plate backed air filled cavity

The first test case to be considered in this paper is a simplified structure, rather than an industrial application. The test structure is a 1 m × 1 m × 0.01 m simply supported aluminium plate, backed by a rigid walled cubic cavity of dimensions 1 m × 1 m × 1 m. The mechanical properties of the structure are as follows: Young's Modulus E = 70 GPa, mass density $\rho_s = 2700$ kg/m^3 and Poisson's ratio $\upsilon = 0.35$. The cubic cavity is filled with air with the following properties: speed of sound $c = 343$ m/s, mass density $\rho_c = 1.2$ kg/m^3. A constant amplitude force excitation of 1 N, over the frequency range from 0 to 300 Hz, was applied at one of the off-center nodes of the structural FE mesh as shown in Figs. 3 and 4. Three hundred and fifty substeps were defined for the analysis. A total of 8400 elements were used for the coupled FE model.

For the solution via the moment-matching approach, 30 Arnoldi vectors were generated using the SISO/SICO Arnoldi process described in the previous section. The noise transfer function (pressure/force) at (0.75 m, 0.75 m,0.25m) and (0.35 m, 0.65 m, 0.30 m) inside the fluid domain are specified as outputs for the analysis. For the MOR via Arnoldi approach, three different expansion points have been chosen: $s = (\omega_E + \omega_B)/4$; $s = (\omega_E + \omega_B)/2; s = \omega_E$. The superimposed noise transfer functions, obtained by ANSYS FE and MOR via Arnoldi for $s = (\omega_E + \omega_B)/2$ are shown in Figs. 5 and 6. It can be observed that there is no visible difference in the respective noise transfer functions. The corresponding local error for all three

[1] The MATLAB benchmark "*bench*" timings for this machine can be found in [30].

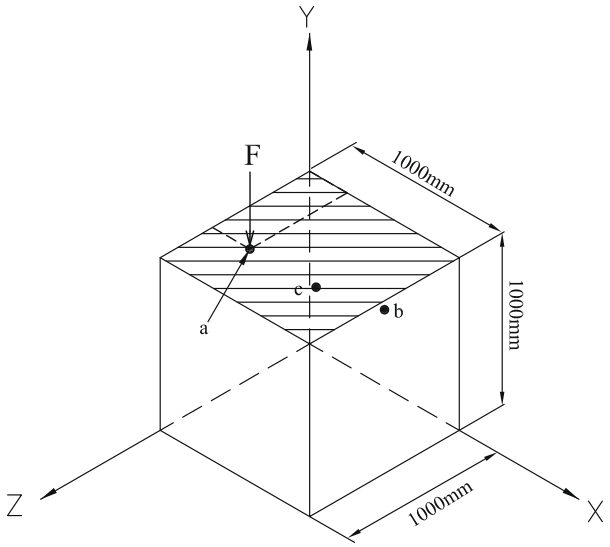

Fig. 3. Plate backed cubic cavity (air filled) system. Excitation location: $a = (0.25\text{ m}, 1\text{ m}, 0.65\text{ m})$; measurement location(s): $b = (0.75\text{ m}, 0.75\text{ m}, 0.25\text{ m})$, $c = (0.35\text{ m}, 0.65\text{ m}, 0.30\text{ m})$.

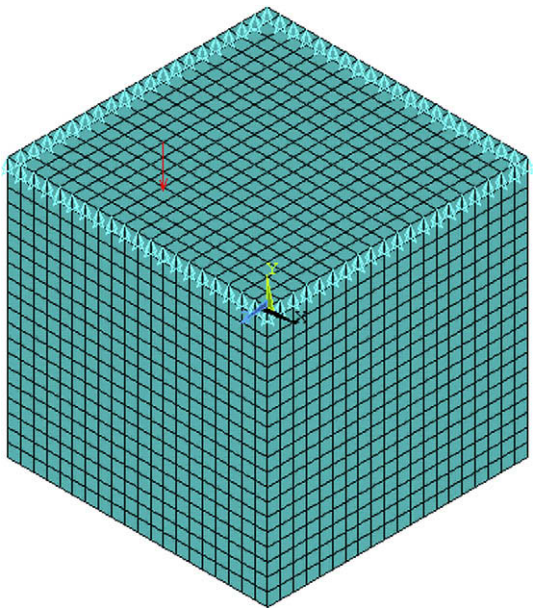

Fig. 4. Test Case No. 1: plate backed by a rigid walled cavity.

expansion points and the *true*, *relative* errors are shown in Figs. 7 and 8 and Fig. 9, respectively. The convergence pattern indicates that to approximate the coupled system to the required level of accuracy required no more than 15 Arnoldi generated vectors for $\omega = 1$ Hz and 30 Arnoldi generated vectors for $\omega = 300$ Hz.

3.1.2. Test Case No. 2: 3D model structure

A simplified vehicle structure, made up of simple beams and plates was generated to provide a more complex test case for the solution of fully coupled undamped systems using MOR based on the Arnoldi algorithm. This solution method was also compared with a harmonic analysis using the direct LU solution method in ANSYS. The FE structural model was divided into seven areas. Two of these areas, which corresponded to the vehicle roof, and front firewall, were meshed using four noded quadrilateral shell elements (ANSYS SHELL181), with six degrees of freedom at each node. The structural model is shown in

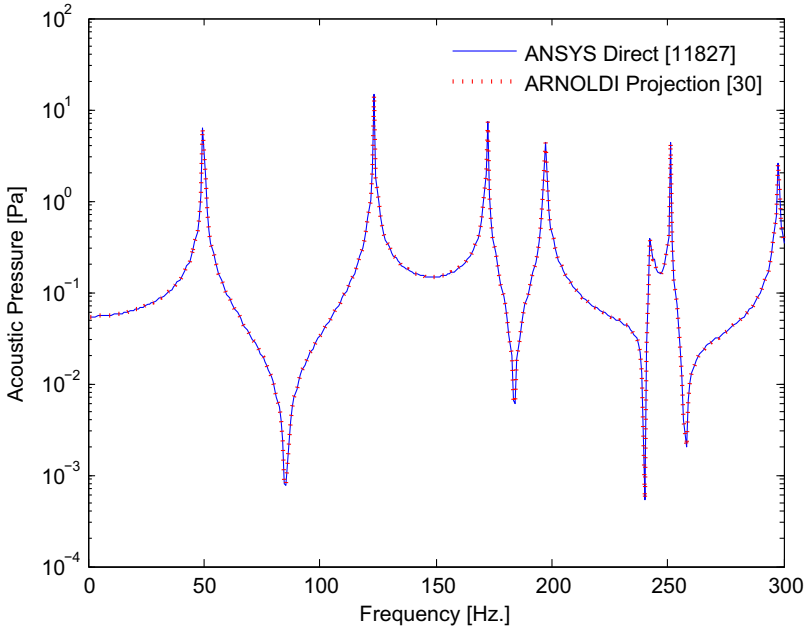

Fig. 5. Test Case No. 1: Predicted noise transfer function using direct and moment-matching Arnoldi projection for fluid node at (0.75 m, 0.75 m, 0.25 m).

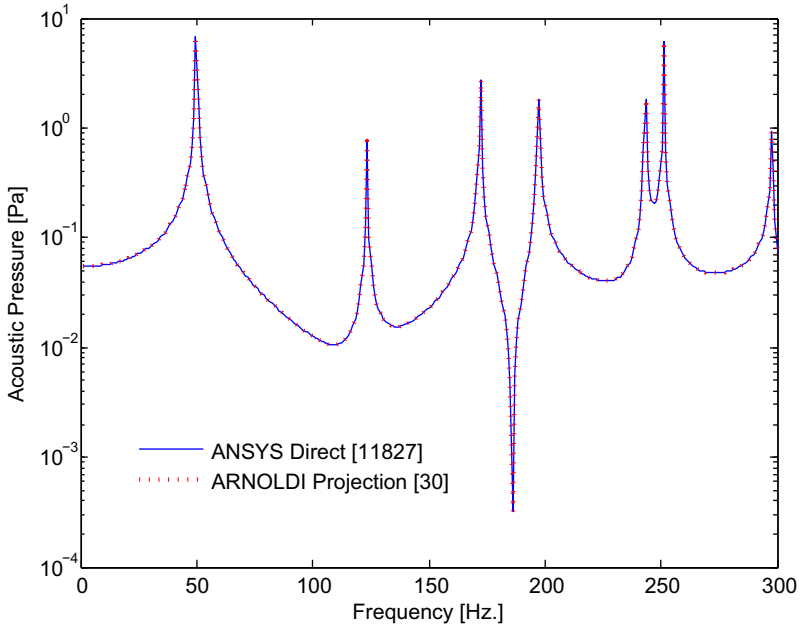

Fig. 6. Test Case No. 1: Predicted noise transfer function using direct and moment-matching Arnoldi projection for fluid node at (0.35 m, 0.65 m, 0.3 m).

Fig. 11. The mechanical properties of the structural elements are as follows: Young's Modulus $E = 200$ GPa, mass density $\rho_s = 7800\ \text{kg/m}^3$ and Poisson's ratio $\upsilon = 0.33$. The enclosed cavity is filled with air with the following properties: speed of sound $c = 343$ m/s, mass density $\rho_c = 1.2\ \text{kg/m}^3$. A total of 692 structural elements – a combination of BEAM4 and SHELL181, were found to be sufficient to capture the dynamic behaviour of the structural model. The acoustic model was modelled using eight-noded acousic brick elements (ANSYS FLUID30), with one pressure degree of freedom at each node. The coupled model is shown in Fig. 12. The structural and acoustic model were coupled using the ANSYS Fluid Structure Interaction (FSI) flag, which in turn creates the *wetted surface* carrying seven degrees of freedom at each node. Faces other

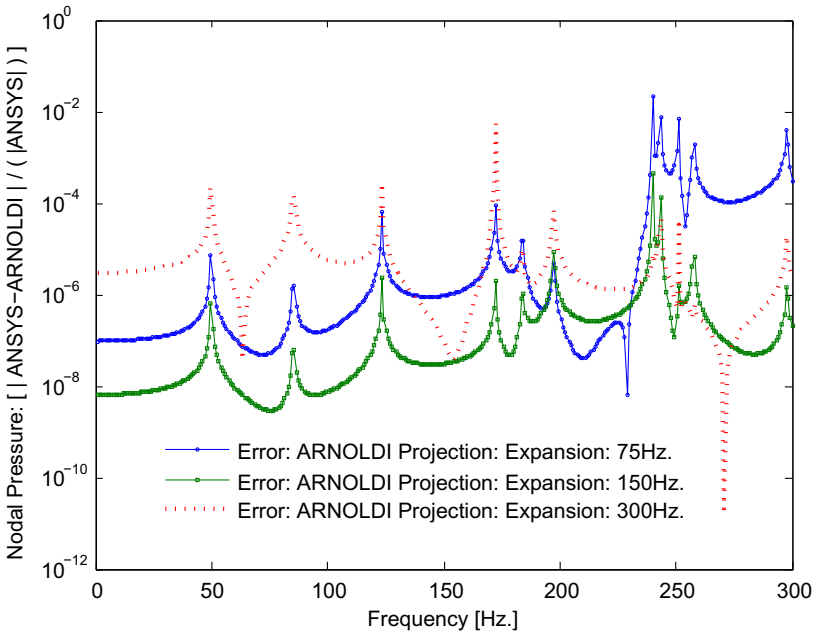

Fig. 7. Test Case No. 1: Noise transfer function error plot for fluid node at (0.75 m, 0.75 m, 0.25 m) for $s = 75$ Hz; $s = 150$ Hz; $s = 300$ Hz.

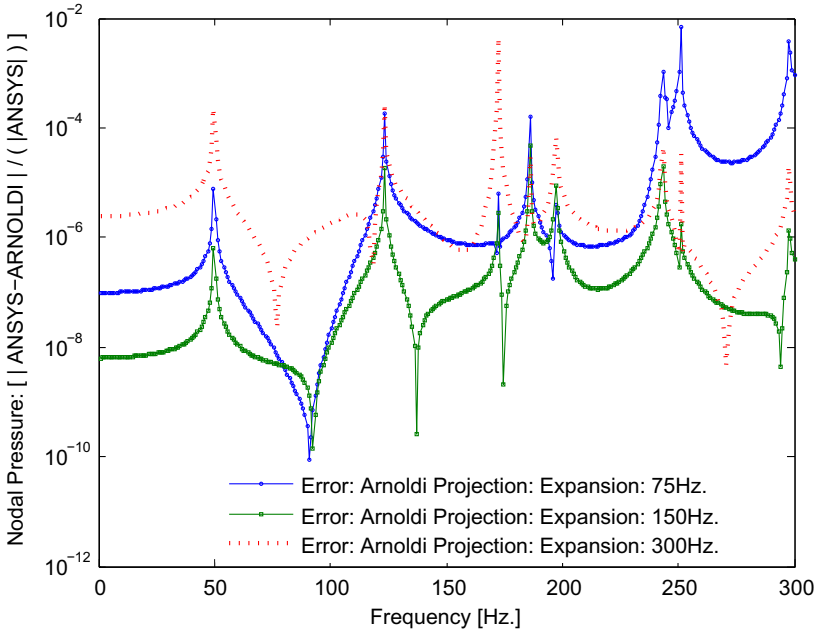

Fig. 8. Test Case No. 1: Noise transfer function error plot for fluid node at (0.35 m, 0.65 m, 0.3 m) for $s = 75$ Hz; $s = 150$ Hz; $s = 300$ Hz.

than the roof and the firewall were assumed to be fully reflective, i.e. rigid walls. The panel thickness range from 1.75 to 2 mm. The coupled model was excited using a constant structural point force of 1 N over the entire frequency range of 0–300 Hz at one of the nodes on the front structural member as shown in Figs. 10–12. In this case study, the beams have been ignored for the coupled model, i.e. the *wetted surface* was not created for the elements belonging to the faces of the beam. The output nodes considered for this test case was representative of front left driver's ear location (0.332 m, 0.38 m, 0.249 m) and at (0.766 m, 0.452 m, 0.249 m).

For the MOR solution method, 150 vectors were generated using the SISO/SICO Arnoldi algorithm implemented in Mathematica. The noise transfer functions at the fluid nodes representative of the drivers ear location (0.33 m, 0.38 m, 0.24 m) and

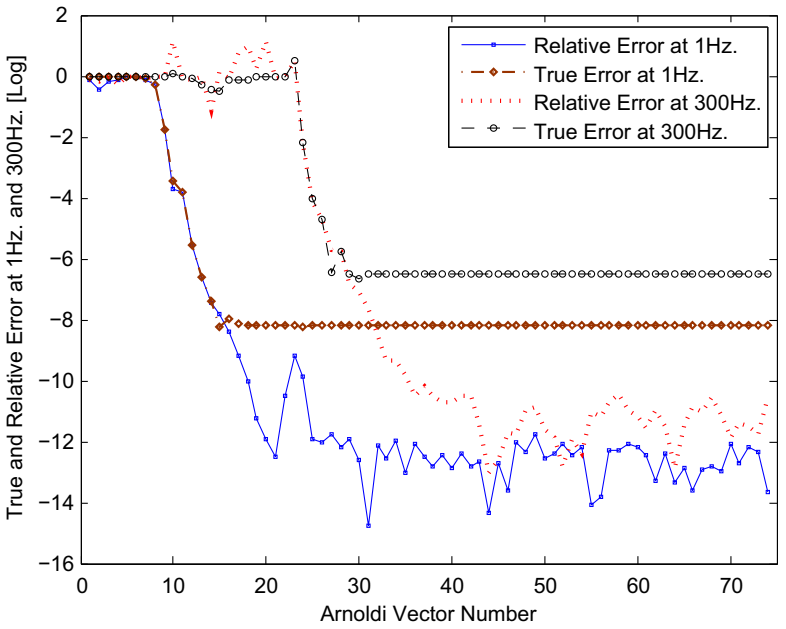

Fig. 9. Test Case No. 1: Convergence pattern for Arnoldi vectors at $\omega = 1$ Hz and $\omega = 300$ Hz.

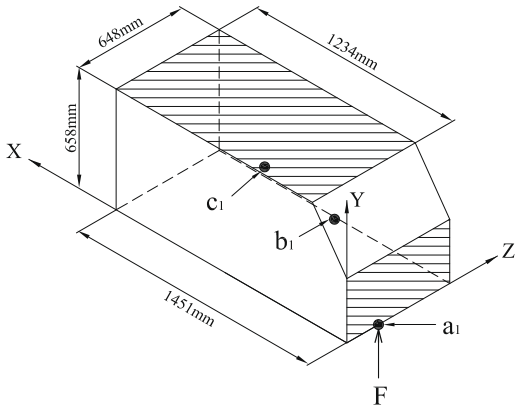

Fig. 10. Beam-plate model structure. Excitation location: $a_1 = (0, 0, 0.2\text{ m})$; measurement location(s): $b_1 = (0.332\text{ m}, 0.38\text{ m}, 0.249\text{ m})$, $c_1 = (0.766\text{ m}, 0.452\text{ m}, 0.249\text{ m})$.

at (0.76 m, 0.45 m, 0.24 m) are shown in Figs. 13 and 14. Similar to *Test Case No.* 1, it can be observed that there is no visible difference in the noise transfer functions obtained via the direct inversion method and the Arnoldi based projection formulation. For the MOR via Arnoldi approach, again, three different expansion points have been chosen: $s = (\omega_E + \omega_B)/4; s = (\omega_E + \omega_B)/2;\ s = \omega_E$. The corresponding local error for all three expansion points and the *true*, *relative* errors are shown in Figs. 15–17, respectively. In this case, The convergence pattern indicates that to approximate the coupled system to the required level of accuracy required no more than 115 Arnoldi generated vectors for $\omega = 1$ Hz and 130 Arnoldi generated vectors for $\omega = 300$ Hz.

3.1.3. Test Case No. 3: 3D plate backed water filled cavity

A plate backed water filled cavity is considered as the third test case to compare the efficiency and accuracy of dimension reduction via the Arnoldi process. This solution method was also compared with a harmonic analysis using the direct LU solution method in ANSYS. The plate is simply supported and has the following dimensions: 0.35 m long, 0.29 m wide, and 0.14 m deep and 0.0015 m thick aluminium plate. The mechanical properties of the structure are as follows: Young's Modulus $E = 72$ GPa, mass density $\rho_s = 2700\text{ kg/m}^3$ and Poisson's ratio $\upsilon = 0.33$. The cavity is filled with water with the following properties: speed of sound $c = 1500\text{ m/s}$, mass density $\rho_c = 1000\text{ kg/m}^3$. The plate is discretized using 18×15 ANSYS SHELL181 elements and the cavity is discretized using $18 \times 15 \times 4$ ANSYS FLUID30 elements. The coupled system

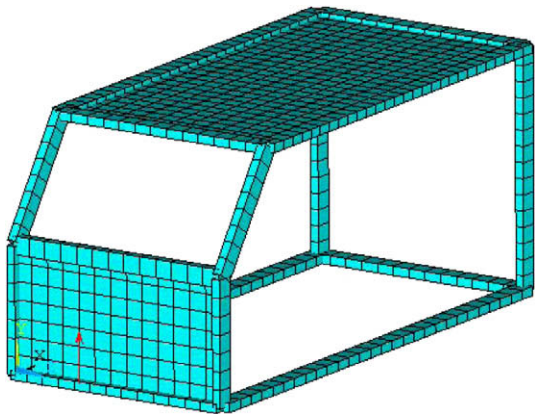

Fig. 11. Test Case No. 2: Structural FE model.

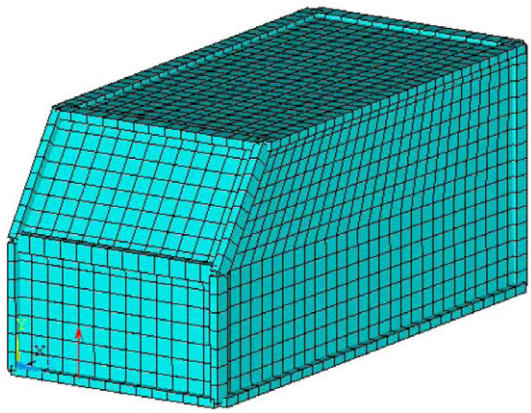

Fig. 12. Test Case No. 2: Coupled structural–acoustic FE model.

was excited using a constant structural point force of 1 N over the entire frequency range of 0–600 Hz at one of the off-center structural nodes on the simply supported plate as shown in Figs. 18 and 19. The desired output quantities considered for this test case are as follows: (a) the structural displacement response at driving point, i.e. at the unit structural point force location $a_2 = (0.039\text{ m}, 0.14\text{ m}, 0.078\text{ m})$ and (b) fluid pressure close to the centre of the rectangular domain at $(0.135\text{ m}, 0.07\text{ m}, 0.175\text{ m})$.

It is worth mentioning that the dimension of the resulting coupled FE model for this test case is indeed small – compared to test cases: (1,2). However, from a modal coupling viewpoint, the presence of a higher density fluid results in a very strong coupling between the plate modes and the cavity modes [18]. Therefore, the test case has been chosen to evaluate the performance of the Arnoldi based projection formulation for *strong coupling*. The sparsity plots for the resulting higher dimensional coupled stiffness and mass matrices are shown in Figs. 20 and 21.

For the MOR solution method, 50 vectors were generated using the SISO Arnoldi algorithm implemented in Mathematica. The noise transfer function and the structural receptance transfer function (structural displacement over structural input force) and the fluid acoustic transfer function (cavity pressure over structural input force) are shown in Figs. 22 and 23. The corresponding fluid pressure and structural displacement errors are shown in Fig. 24. For the MOR via Arnoldi approach, an expansion point of $s = \omega = 350$ Hz was used. The convergence plot at $s = \omega = 1$ Hz and $s = \omega = 600$ Hz obtained via Eqs. (51) and (52) is shown in Fig. 25. It can be observed that to approximate the coupled system to the required level of accuracy required no more than 50 Arnoldi generated vectors for both $\omega = 1$ Hz and for $\omega = 600$ Hz.

3.2. Discussion of numerical results

The three test cases used in this paper, show that good approximation properties can be obtained by projecting a higher dimensional system to a lower dimension and matching the low frequency moments of the system. For test cases (1,2), the moments are matched at three different expansion points $s = (\omega_E + \omega_B)/4;\ s = (\omega_E + \omega_B)/2;\ s = \omega_E$, to analyze the effect of moment matching and its resulting accuracy.

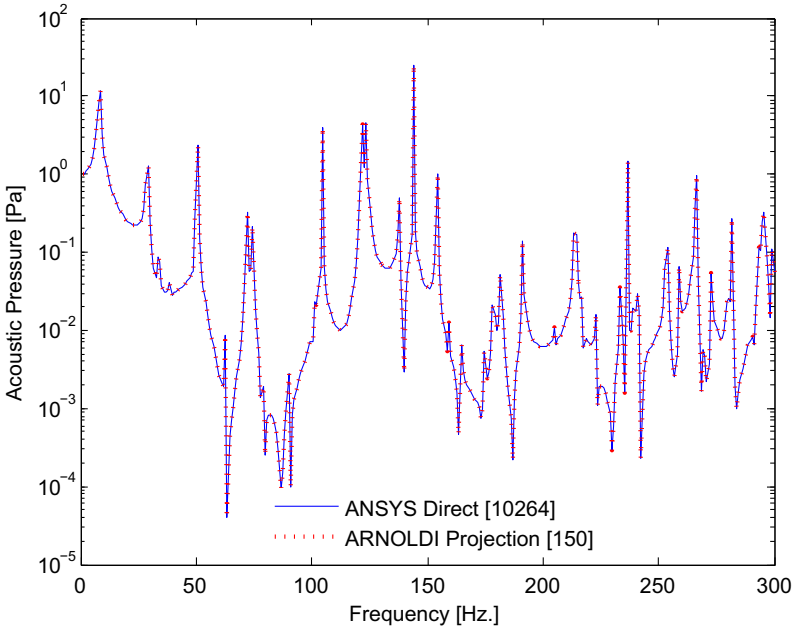

Fig. 13. Test Case No. 2: Predicted noise transfer function using direct and moment-matching Arnoldi projection for fluid node at (0.332 m, 0.38 m, 0.249 m).

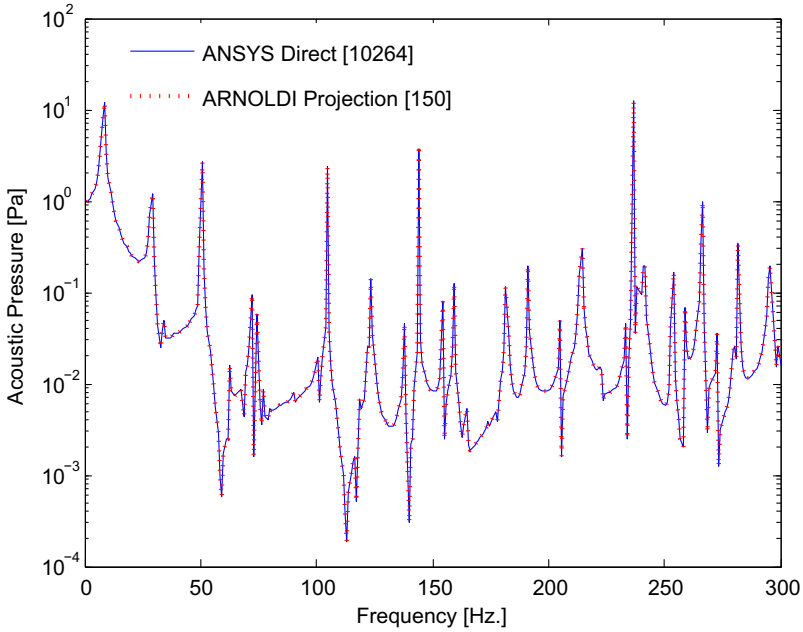

Fig. 14. Test Case No. 2: Predicted noise transfer function using direct and moment-matching Arnoldi projection for fluid node at (0.766 m, 0.452 m, 0.249 m).

The choice of s (expansion points) is often an open question [34], and depends on the nature of the coupled problem under investigation. If a Taylor series expansion is considered around a higher frequency, a reduced order model could be obtained with better approximation properties around that frequency range. In this test cases shown, it can be seen that matching the moments around a particular expansion point, results in a more accurate lower dimensional model around that chosen particular frequency, i.e. the error in the frequency domain, between the higher dimensional and lower dimensional model tends to grow away from the expansion point. In *Test Case No.* 1, for expansion points of $s = (\omega_E + \omega_B)/4$ and $s = \omega_E$, it can be observed that, the maximum error is approximately in the order of 10^{-6} at 150 Hz and 10^{-2} at 300 Hz, respectively.

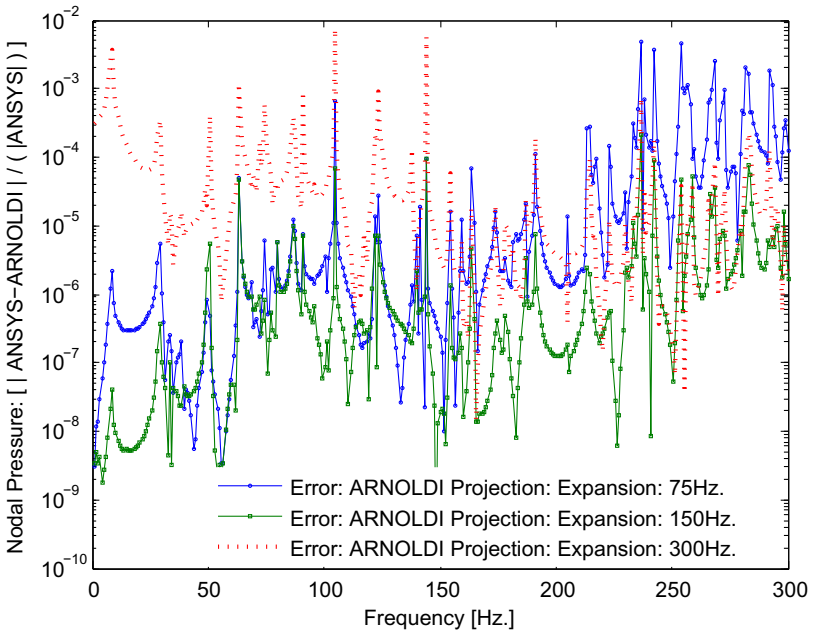

Fig. 15. Test Case No. 2: Noise transfer function error plot for fluid node at (0.33 m, 0.38 m, 0.24 m) for $s = 75$ Hz; $s = 150$ Hz; $s = 300$ Hz.

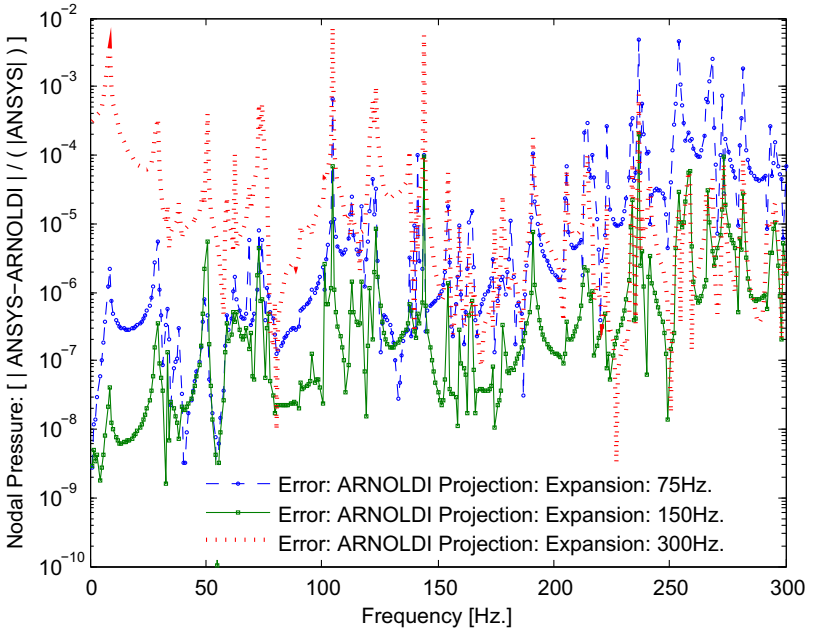

Fig. 16. Test Case No. 2: Noise transfer function error plot for fluid node at (0.76 m, 0.45 m, 0.24 m) for $s = 75$ Hz; $s = 150$ Hz; $s = 300$ Hz.

However, for an expansion point of $s = (\omega_E + \omega_B)/2$ it can be observed the maximum error is in the order of 10^{-3} at 150 Hz. In general, it can be observed that, a higher accuracy is obtained when the moments are matched at half the analysis range. This higher accuracy can be attributed to the fact that, the moments are matched at around half the analysis range leading to a lower dimensional model sufficient enough to well represent both the frequency bands of 0–150 Hz and 150–300 Hz.

Similarly, for *Test Case No.* 2, for expansion points of $s = (\omega_E + \omega_B)/4$ and $s = \omega_E$, it can be observed from Figs. 15 and 16 that, the maximum error is in the order of 10^{-2} at 300 Hz and 10^{-2} at ~100 Hz, respectively. This general trend can be observed for all three fluid output nodes considered in this paper. Again, it can be observed that, for an expansion point of $s = (\omega_E + \omega_B)/2$ the maximum error is in the order of 10^{-4} at 150 Hz, i.e. a higher accuracy can is obtained if an expansion

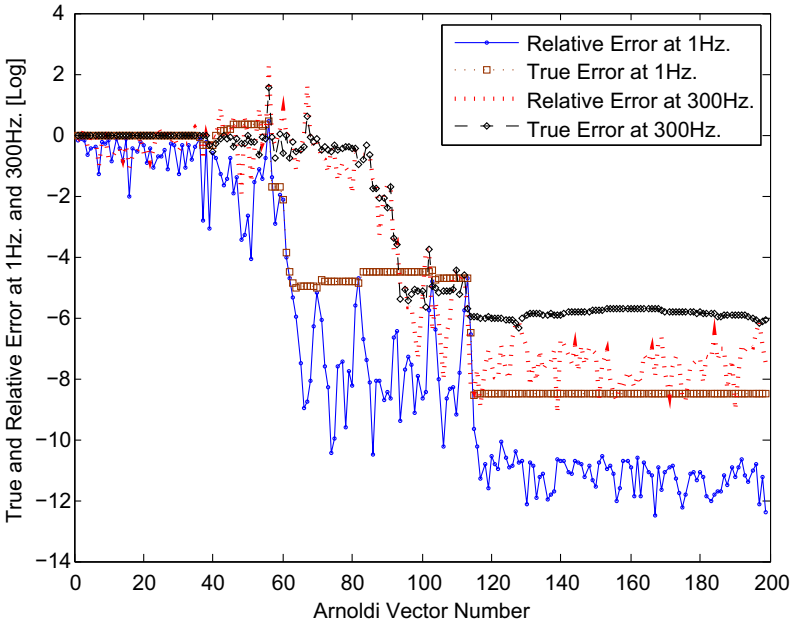

Fig. 17. Test Case No. 2: Convergence pattern for Arnoldi vectors at $\omega = 1$ Hz and $\omega = 300$ Hz.

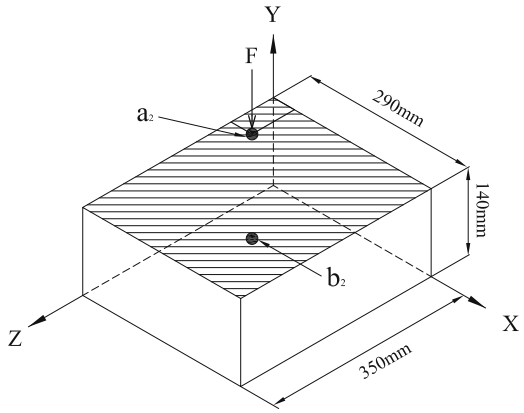

Fig. 18. Test Case No. 3: Plate backed rectangular cavity (water filled) system. Excitation location: $a_2 = (0.039\text{ m}, 0.14\text{ m}, 0.078\text{ m})$; measurement location(s): $a_2 = (0.039\text{ m}, 0.14\text{ m}, 0.078\text{ m})$, $b_2 = (0.135\text{ m}, 0.07\text{ m}, 0.175\text{ m})$.

point equal to half the analysis range is used to generate the Arnoldi vectors. Figs. 5 and 6 indicate that the reduced order model accurately captures the dynamic behavior of the coupled higher dimensional system, indicated by peaks at ~170 Hz and ~240 Hz, which correspond to the second and third acoustic mode of the cavity in the frequency range of 0–300 Hz. In addition to simply matching moments at one distinct expansion point, a reduced order model via the Arnoldi process, could be computed, which matches moments around several expansion points, with each expansion point requiring a separate factorization, leading to rational Krylov Subspace methods. However, for the test cases analyzed in this paper, a single expansion point seems to yield very good approximation properties. Figs. 5, 6, 15, 16, 22, 23 indicate that there is almost no difference between the higher dimensional model solved using the direct LU method for each defined substep and the reduced order model generated via implicit moment matching. In addition to this, a complete approximation of the output is specific to the Arnoldi process [50].

While there exists several methods to choose basis vectors, such as coupled or uncoupled (individually for the structural and the fluid domain) eigen vectors, in this work we have chosen these *projection* vectors to span the Krylov Subspace. Compared to the computing eigen modes and eigen vectors of the system matrices, computing vectors spanning the Krylov Subspace is much faster and efficient, since a normal modal analysis of a complex structural or an acoustic system tends to be computationally expensive. In addition to this, if modal contribution factors are required, a coupled eigen value problem has to be solved using an unsymmetric eigen value solver, leading to further inefficiency in the calculation procedure. In fact,

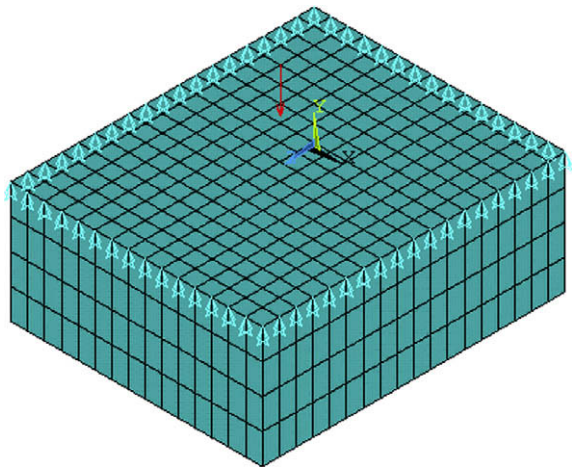

Fig. 19. Test Case No. 3: Fully coupled FE model.

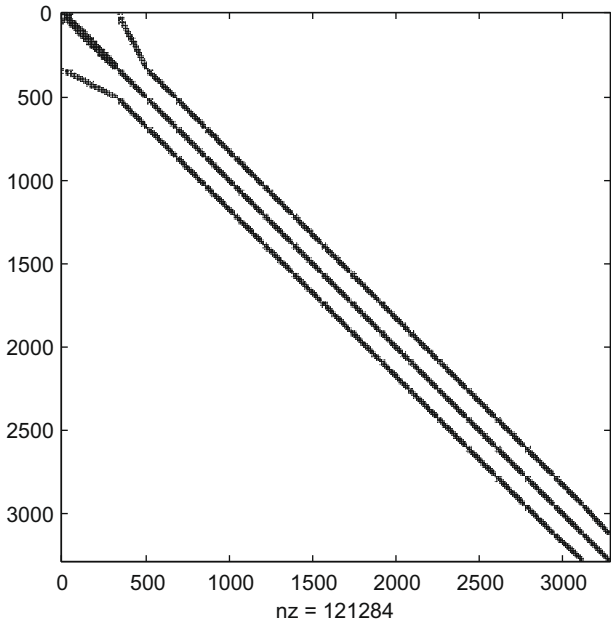

Fig. 20. Test Case No. 3: Stiffness matrix sparsity plot.

there is no guarantee that the computed modes included for the mode superposition would be enough to obtain a required degree of accuracy. Often $1.2\omega_e - 2\omega_e$ modes are computed for projection as an estimate, ω_e being the analysis end frequency range [51,16]. Infact, for an acoustic constantly damped version of *Test Case No.* 3, it has been observed that the fluid and structural state variables do not converge in spite of retaining 50 structural and acoustic modes respectively [18]. To counter this problem, pseudostatic corrections have been proposed [52,17,18]. For the Arnoldi based projection approach, it can be seen from Fig. 24 that the relative errors for the considered fluid and structural transfer functions converge with 45 Arnoldi generated vectors for a coupled dynamic matrix expanded at $s = 350$ Hz. In this case, the maximum fluid and structural error is in the order of 10^{-5}. Further, this also indicates that with the moment-matching via the Arnoldi framework, it is possible to evaluate for both field states simultaneously, which in this case are fluid pressures and structural displacements.

The overall computational times for Test Case Nos. 1–3 are shown in Table 1. A breakdown of computational times involved in the set-up and solving a ROM via the Arnoldi process is shown in Table 2. It can be seen that significant speed up (∼95%) is achieved by employing order reduction via the Arnoldi process. Further, the reduction seems consistent in all three test cases. The number of vectors needed to accurately represent the system were calculated using Eqs. (51) and

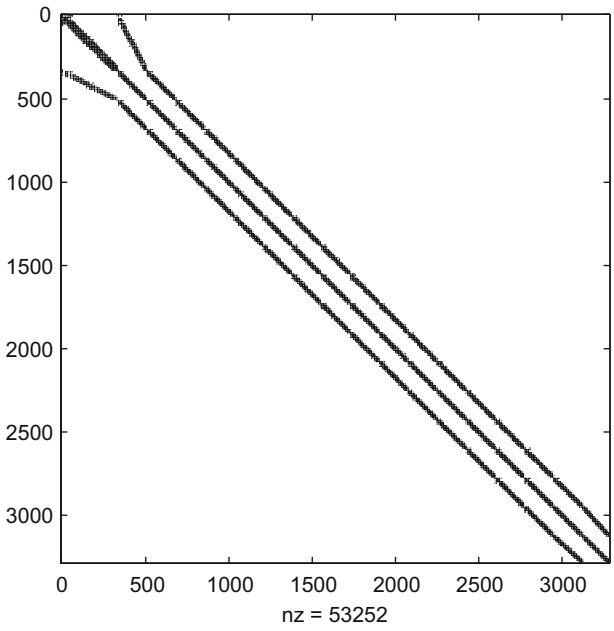

Fig. 21. Test Case No. 3: Mass matrix sparsity plot.

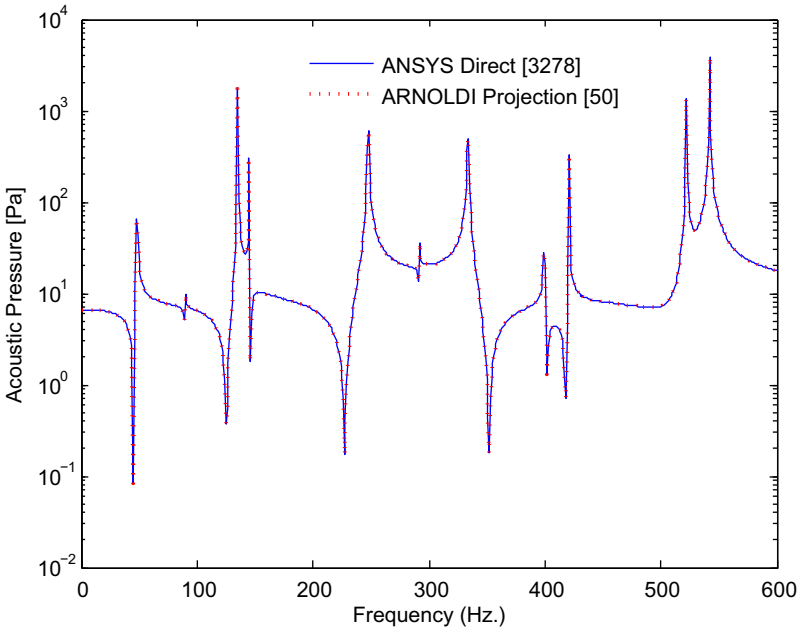

Fig. 22. Test Case No. 3: Predicted fluid noise transfer function using direct and moment-matching Arnoldi projection for fluid node at (0.038 m, 0.14 m, 0.077 m).

(52). It was shown that the order of the Arnoldi vectors needed to accurately represent the system were 30, 150 and 50 for test cases 1, 2 and 3 respectively. At this point, machine precision was reached, using 16 significant digits for processing outputs of both the higher dimensional and the reduced order model and therefore a further better approximation could not be found. The number of vectors required to adequately approximate the transfer function, depends on the model size, the number of inputs specified to excite particular modes of the system, and the frequency band under investigation. In the described one-sided Arnoldi process the output does not participate in the reduction process, and so the approximation is completely independent of the number and location of outputs specified. It is also worth noting that the process of computing the number of required vectors, can be completely automated using an user defined parameter.

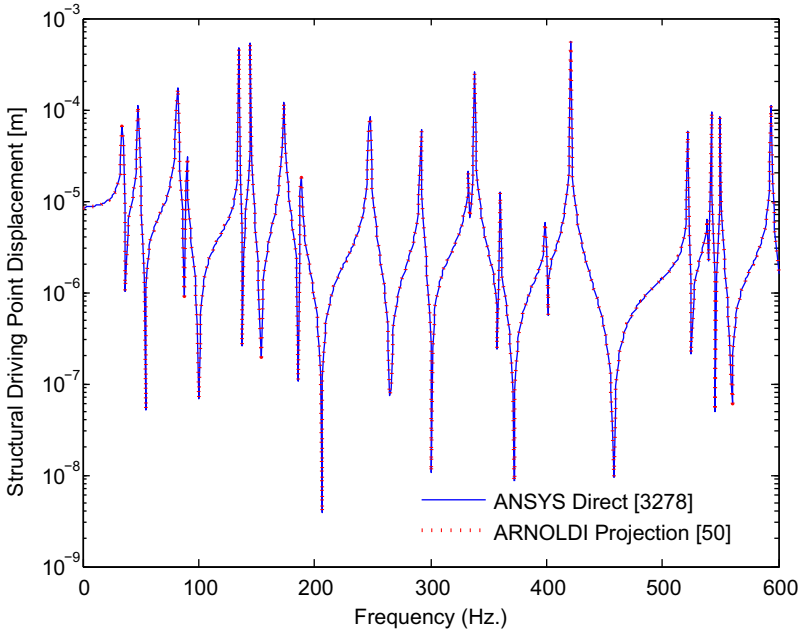

Fig. 23. Test Case No. 3: Predicted structural receptance transfer function using direct and moment-matching Arnoldi projection for fluid node at (0.33 m, 0.38 m, 0.24 m).

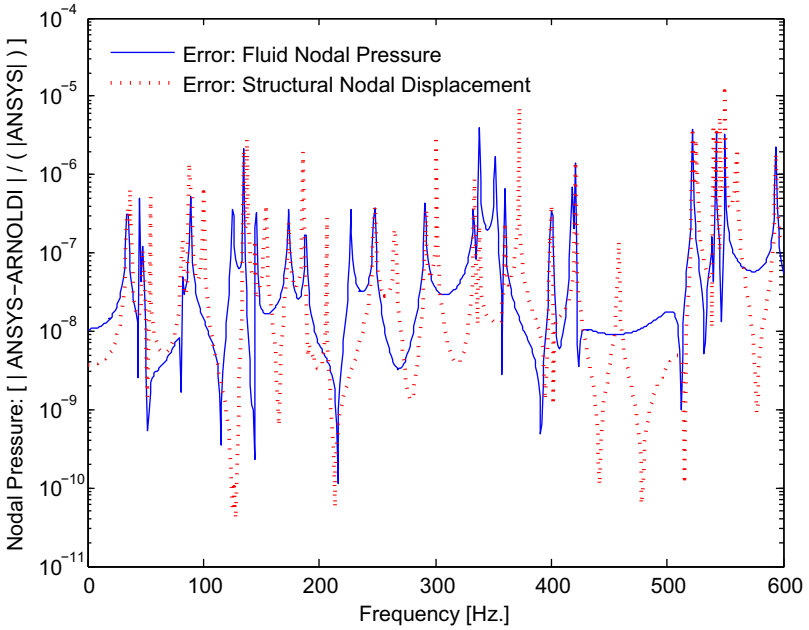

Fig. 24. Test Case No. 3: Error plot for fluid and structural outputs.

4. Conclusion

A new method to develop a more efficient reduced order model for fully coupled structural–acoustic problems has been outlined. The basis vectors for model reduction are computed by applying the Arnoldi algorithm, which computes the projection vectors spanning the Krylov Subspace, to match the maximum number of moments of the system. In this work, for the first two test cases considered, air has been used as a fluid medium, given that the application of interest is noise and vibration of automotive/aerospace type structures. In addition to this, as the third numerical test case, a water filled rectan-

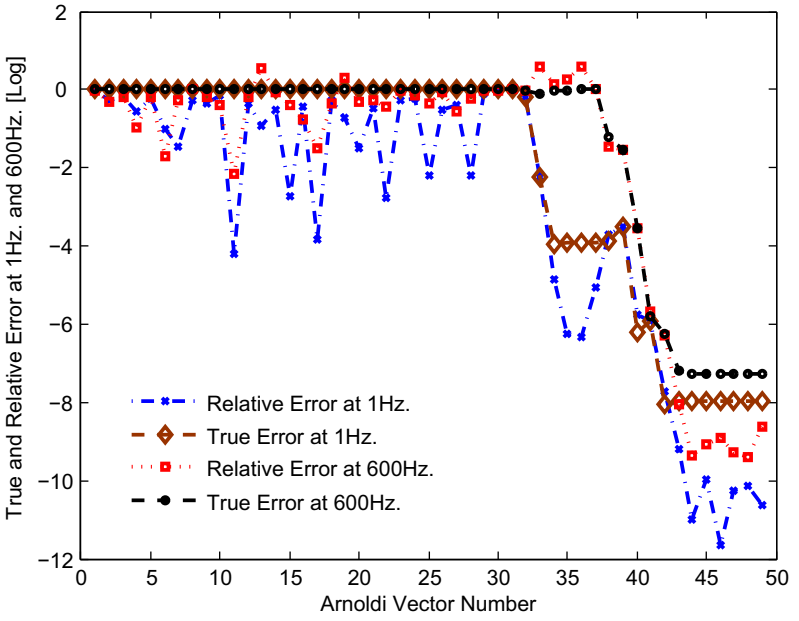

Fig. 25. Test Case No. 3: Convergence pattern for Arnoldi vectors at $\omega = 1$ Hz and $\omega = 300$ Hz.

Table 1
A comparison of overall computational times.

Test case DOF's	ANSYS direct (s)	ROM via Arnoldi (s)	Time reduction (%)
11,827[a]	8933.2	301.5	96.62
10,264[b]	5208.5	289.8	94.43
3278[c]	2435	82.73	96.60

[a] Test Case No. 1
[b] Test Case No. 2
[c] Test Case No. 3

Table 2
Breakdown of computational times.

Test case	Computational steps: ROM via Arnoldi	Time (s)
Extract matrices	ANSYS static solution (ANSYS)	10.3[a] [2]9.2[b] [3]4[c]
	Extract matrices (ANSYS/*mor4fem*)	231.5[a] 203.4[b] 64.76[c]
TC:1 : 3D air filled cavity	Read matrices (mathematica)	23.1
	Vector computation and projection (mathematica)	36
	Harmonic analysis and convergence (mathematica/MATLAB)	0.6
	Total: ROM via Arnoldi	**301.5**
TC:2 : 3D model structure	Read matrices (mathematica)	20
	Vector computation and projection (mathematica)	51.6
	Harmonic analysis and convergence (mathematica/MATLAB)	5.6
	Total: ROM via Arnoldi	**289.8**
TC:3 : 3D water filled cavity	Read matrices (mathematica)	1
	Vector computation and projection (mathematica)	7.10
	Harmonic analysis and convergence (mathematica/MATLAB)	5.87
	Total: ROM via Arnoldi	**82.73**

[a] Test Case No. 1.
[b] Test Case No. 2.
[c] Test Case No. 3.

gular cavity was used to demonstrate the applicability of moment-matching based Arnoldi formulation to strongly coupled structural–acoustic problems. It was also shown that it is possible to match both displacements on the structure and pressure levels in the fluid. For more complex test cases involving water filled cavities and Benchmark type problems for fully coupled structural–acoustics, the reader is referred to [53,30].

A straightforward extension of the projection framework presented in this paper can also be made for constant structural or acoustic damping via the well known complex stiffness approach. Other alternatives to modelling damping within the Arnoldi projection framework involve transforming the coupled system to first order and applying moment matching algorithms or by utilizing higher order Arnoldi methods. The method described in this paper could serve as an excellent alternative to many other reduction techniques, particularly for vibro-acoustic optimization, where reduction of computational time is often required. In terms of future work, generating reduced order models via implicit moment matching could be extended to the analysis of constant or frequency dependent structural/acoustic damping and to other vehicle/aerospace NVH related applications such as contribution analysis and element level sound pressure computations which often take the form of objective functions for coupled structural–acoustic sensitivity or optimization analysis.

Acknowledgements

The first authors wish to acknowledge the Engineering and Physical Sciences Research Council (EPSRC GR/S27245/01) for the grant project under which this research was carried out. The first authors also acknowledge the support of T. Bharj (Ford Motor Company UK), M. Birrell (BI-Composites, UK), R. Davidson (Crompton Technology, UK), M. Collier (Hodgson and Hodgson, UK), A. Atkins (Siemen's Magnet Technology, UK) and M. Burnett (Motor Industry Research Association, UK) who were industrial collaborators in the project.

References

[1] O.C. Zienkiewicz, R. Newton, Coupled vibrations of a structure submerged in a compressible fluid, in: Proceedings of the International Symposium on Finite Element Techniques, vol. 15, 1969, pp. 1–15.
[2] A. Craggs, The transient response of a coupled plate-acoustic system using plate and acoustic finite elements, J. Sound Vibrat. 15 (1971) 509–528.
[3] A. Craggs, An acoustic finite element approach for studying boundary flexibility and sound transmission between irregular enclosures, J. Sound Vibrat. 30 (1973) 343–357.
[4] N. Atalla, R.J. Bernhard, Review of numerical solutions for low frequency structural–acoustic problems, Appl. Acoust. 43 (5) (1994) 271–294.
[5] J.A. Wolff, Modal synthesis for combined structural acoustic system, AIAA J. 15 (1977) 743–745.
[6] W. Desmet, A wave based prediction technique for coupled vibro-acoustic analysis, Ph.D. Thesis, Department of Mechanical Engineering, Katholieke Universiteit Leuven, Belgium, 2003.
[7] W. Desmet, D. Vandepitte, Advanced numerical acoustics: the finite element method, Course notes ISAAC 2005: Advanced Numerical Acoustics, vol. 1(1), 2005, pp. 01–208.
[8] G.C. Everstine, A symmetric potential formulation for fluid structure interactions, J. Sound Vibrat. 79 (1981) 157–160.
[9] L.G. Olson, K.J. Bathe, Analysis of fluid structure interactions: a direct symmetric coupled formulation based on fluid velocity potential, Comput. Struct. 21 (1985) 21–32.
[10] H. Morand, R. Ohayon, Substructure variational analysis of the vibrations of coupled fluid structure systems, Int. J. Numer. Methods Eng. 14 (4) (1979) 741–755.
[11] G.C. Feng, L. Kiefling, Fluid structure finite element vibrational analysis, J. Aircraft Eng. Aerospace Technol. (1976) 199–203.
[12] X. Wang, K.J. Bathe, Displacement/pressure based mixed finite element formulations for acoustic fluid structure interaction problems, Int. J. Numer. Methods Eng. 40 (1997) 2001–2017.
[13] R. Pirk, W. Desmet, B. Pluymers, P. Sas, L.C.S. Goes, Vibro-acoustic analysis of the Brazilian vehicle satellite launcher (VLS) fairing, in: Proceedings of the ISMA'2002 International Conference on Noise and Vibration Engineering, vol. 2, 2002, pp. 2075–2085.
[14] S. Marburg, Developments in structural–acoustic optimization for passive noise control, Arch. Comput. Methods Eng. 9 (4) (2002) 291–370.
[15] C. Pal, I. Hagiwara, Dynamic analysis of a coupled structural–acoustic problem: simulatneous multi-modal reduction of vehicle interior noise level by combined optimization, Finite Elem. Eng. Des. 14 (1993) 21–32.
[16] S. Boily, F. Charron, The vibroacoustic response of a cylindrical shell structure with viscoelastic and poroelastic materials, J. Appl. Acoust. 58 (2) (1999) 131–152.
[17] R. Ohayon, C. Soize, Structural Acoustics and Vibration, first ed., Academic Press, 1998. ISBN-13: 978-0125249454.
[18] M. Tournour, N. Atalla, Pseudostatic corrections for the forced vibroacoustic response of a structure–cavity system, J. Acoust. Soc. Am. 107 (5) (2000) 2379–2386.
[19] R. Ohayon, Reduced models for fluid–structure interaction problems, Int. J. Numer. Methods Eng. 60 (2004) 139–152.
[20] S. Kim, J. Lee, M.H. Sung, Structural acoustic modal coupling analysis and application to noise reduction in a vehicle passenger compartment, J. Sound Vibrat. 225 (5) (1999) 989–999.
[21] H. Morand, R. Ohayon, Fluid Structure Interaction, first ed., John Wiley and Sons and Ltd., 1995. ISBN-13: 978-0471944591.
[22] ABAQUS, V6.5 Theory and Benchmark Manual, 2005. <http://www.simulia.com/>.
[23] J.K. Bennighof, Vibroacoustic frequency sweep analysis using automated multi-level substructuring, in: 40th AIAA/ASME/ASCE/AHS/ASC Structures, Structural Dynamics, and Materials Conference and Exhibit, vol. 1, 1999, pp. 1–6.
[24] S. Marburg, H.J. Hardtke, R. Schmidt, D. Pawandenat, Application of the concept of acoustic influence coefficients for the optimization of a vehicle roof, Eng. Anal. Bound. Elem. 20 (4) (1997) 305–310.
[25] Sysnoise, V5.5 Theory Manual, 2004. <http://www.lmsintl.com>.
[26] M. Malhotra, P.M. Pinsky, Efficient computation of multi-frequency far-field solutions of the Helmholtz equation using Padé approximation, J. Comput. Acoust. 6 (1) (2000) 223–240.
[27] M.M. Wagner, P. M Pinsky, A. Oberai, Application of Padé via Lanczos approximations for efficient multifrequency solution of Helmholtz problems, J. Acoust. Soc. Am. 113 (1) (2003) 313–319.
[28] W. Desmet, D. Vandepitte, Mid-frequency vibro-acoustic modelling: challenges and potential solutions, in: Proceedings of the ISMA'2002 International Conference on Noise and Vibration Engineering, vol. 2(1), 2002, pp. 835–862.
[29] L.L. Thompson, A review of finite-element methods for time-harmonic acoustics, J. Acoust. Soc. Am. 119 (3) (2006) 1315–1330.
[30] R.S. Puri, Krylov Subspace Based Direct Projection Techniques For Low Frequency, Fully Coupled, Structural Acoustic Analysis and Optimization, Ph.D. Thesis, School of Technology, Department of Mechanical Engineering and Mathematical Sciences, Oxford Brookes University, Oxford, UK, 2008.

[31] S. Marburg, B. Nolte, (Eds.), Computational Acoustics of Noise Propagation in Fluids - Finite and Boundary Element Methods, XIV, 578p. Springer, 2008. ISBN: 978-3-540-77447-1.
[32] Z.J. Bai, Krylov Subspace techniques for reduced order modeling of large scale dynamical systems, Appl. Numer. Math. 43 (2002) 9–44.
[33] R.W. Freund, Krylov Subspace methods for reduced order modeling in circuit simulation, J. Appl. Math. 123 (2000) 395–421.
[34] A.C. Antoulas, Approximation of large-scale dynamical systems, Society for Industrial and Applied Mathematics, first ed., 2003. ISBN 0-89871-529-6.
[35] T. Bechtold, E.B. Rudnyi, J.G. Korvink, Fast Simulation of Electro-Thermal MEMS: Efficient Dynamic Compact Models. Springer Series: Microtechnology and MEMS, first ed., 2006. ISBN-10: 3-540-34612-0.
[36] K. Willcox, J. Peraire, J. White, An Arnoldi approach for generation of reduced-order models for turbomachinery, Comput. Fluids 31 (2002) 369–389.
[37] G. Lassaux, High-fidelity reduced-order aerodynamic models: Application to active control of engine inlets, Master's Thesis, Department of Aeronautics and Astronautics, Massachusetts Institute of Technology, 2002.
[38] E.B. Rudnyi, J.G. Korvink, Review: Automatic model reduction for transient simulation of MEMS-based devices, Sensors Update 11 (2002) 3–33.
[39] ANSYS, V10 Theory Manual, 2005. <http://www.ansys.com>.
[40] K.J. Bathe, Finite Element Procedures, first ed., Prentice-Hall, Englewood Cliffs, 1995. ISBN 0-13-301458-4.
[41] T.J. Su, R.R. Craig, Krylov model reduction algorithm for undamped structural dynamics systems, AIAA J. Guidance Control Dynam. 14 (1991) 1311–1313.
[42] F.J. Fahy, Foundations of Engineering Acoustics, first ed., Academic Press, 2000. ISBN 0-12247-665-4.
[43] K. Gallivan, E. Grimme, P. Van Dooren, Asymptotic waveform evaluation via a Lanczos method, Appl. Math. Lett. 5 (7) (1994) 75–80.
[44] P. Feldmann, R.W. Freund, Efficient linear circuit analysis by Padé approximation via the Lanczos process, IEEE Trans. Comput.-Aid. Des. Integr. Circuits Syst. 1 (1995) 639–649.
[45] R.W. Freund, Model reduction methods based on Krylov Subspaces, Acta Numerica 12 (1) (2003) 267–319.
[46] R.W. Freund, M.H. Gutknecht, N.M. Nachtigal, An implementation of the look-ahead Lanczos algorithm for non-hermitian matrices, J. Sci. Comput. 15 (1994) 313–337.
[47] Z. Bai, P. Feldmann, R.W. Freund, Stable and passive reduced-order models based on partial Padé approximation via the Lanczos process, Numerical Analysis Manuscript No. 97-3-10, 1997. Available online from <http://cm.bell-labs.com/cs/doc/97>.
[48] V. Simoncini, D.B. Szyld, Recent computational developments in Krylov Subspace methods for linear systems, Numer. Linear Algebra Appl. 14 (2007) 01–59.
[49] E.B. Rudnyi, J.G. Korvink, Model order reduction for large scale engineering models developed in ANSYS, Lect. Notes Comput. Sci. 3732 (2006) 349–356.
[50] T. Bechtold, E.B. Rudnyi, J.G. Korvink, Automatic generation of compact electro-thermal models for semiconductor devices, IEICE Trans. Electron. E86C (3) (2003) 459–465.
[51] E.L. Wilson, M.W. Yuan, J.M. Dickens, Dynamic analysis by direct superposition of Ritz vectors, Int. J. Earthquake Eng. Struct. Dynam. 19 (1982) 813–821.
[52] O.E. Hansteen, K. Bell, On the accuracy of mode superposition analysis in structural dynamics, Int. J. Earthquake Eng. Struct. Dynam. 7 (1979) 405–411.
[53] R.S. Puri, D. Morrey, J.L. Cipolla, A comparison between one-sided and two-sided Arnoldi based model order reduction techniques for fully coupled structural acoustic analysis, in: 153rd Meeting of the Acoustical Society of America, The Journal of Acoustical Society of America, vol. 121(5), 2007.